

The effect of temperature on the permeability of a porous material

WILLARD W. PULKRABEK

Department of Mechanical Engineering, University of Wisconsin-Platteville, Platteville, WI 53818, U.S.A.

and

WARREN E. IBELE

Department of Mechanical Engineering, Heat Transfer Laboratory, University of Minnesota, Minneapolis, MN 55455, U.S.A.

(Received 7 July 1986 and in final form 2 October 1986)

Abstract—The effect of temperature on the flow of compressible fluids through consolidated porous media has been studied experimentally. The work covers a temperature range of 255–1520 K at a pressure of 1 atm. The porous medium was aluminum oxide ceramic with a porosity range of 38.1–49.8%. The gases studied were air, nitrogen, helium and argon. In particular the effect of the ‘slip’ correction term used to explain the change in permeability in the porous flow equations was studied. This permeability correction term depends on the mean free path of the gas and would be expected to increase with temperature. Also the observed permeability should be different for each gas, due to the molecular diameter dependency of the mean free path according to kinetic theory. Both of these expectations were found consistent with the microscopic assumptions. Plots are given showing the relationship of permeability and temperature for the four gases. Helium behavior departs from that of the other three gases. Also shown is how the porous material parameters vary with temperature.

INTRODUCTION

WHEN compressible fluids flow through consolidated porous media the flow equations are modified to include a term allowing for molecular slip in the pores of the solid media. When the pressure is low enough, or the pore size small enough, the mean free path of the molecules is of the same order as the diameters of some of the pores. Under these circumstances a greater mass flow rate than would be expected on the basis of pressure drop measurement occurs, as in the case of fluid flow through a capillary tube. The flow equation for the motion of fluids in a capillary tube is modified for slip flow by a correction term containing the mean free path of the gas. A similar correction term when added to the porous flow equation brings agreement with experiment when the constants are suitably adjusted.

A number of investigators [1–5] have tested this correction term for the porous flow equation and found it to be consistent with experimental evidence. These studies examined the influence of pressure variation over a significant range, while the temperature remained constant at approximately 20°C. At constant temperature the mean free path of a gas varies inversely with pressure, as does the correction term, which is in accord with the experimental results. The phenomenon of slip flow and its effect on the porous flow equation is thus understood at room temperature.

Of late, compressible flow in consolidated porous media has occurred in a number of applications. These

include the mass transfer cooling of aerodynamic surfaces and turbine blades, flow in catalytic converters, and gas injection into the arc region of high-temperature plasmas. In such applications an accurate characterization of the flow of compressible fluid through consolidated porous media at high temperatures is needed, yet scant experimental data are available for predicting the temperature dependence of the flow parameters in porous flow. The only data available [2, 5–9] is in the range of 0–60°C.

The purpose of this work is the measurement of the temperature dependence of the flow properties of a porous medium. The temperature ranged from 255 to 1520 K at a constant pressure of 1 atm.

THE FLOW OF FLUIDS THROUGH POROUS MEDIA

The modern equations for flow through porous media date from 1856, when Darcy first studied water flowing through beds of sands. In differential form Darcy's flow equation can be written as

$$-k \frac{dP}{ds} = \mu V \quad (1)$$

where dP is the differential change in pressure over lengths ds , μ the dynamic viscosity, and V the fluid velocity. This equation defines the constant k , the permeability of the porous medium. The permeability is conceived to be a property of the solid porous medium, independent of the flowing fluid, and de-

NOMENCLATURE

A	cross-sectional area of flow [m^2]	P_0	pressure of 1 atm
B	material parameter [m^{-1}]	R	gas constant [$\text{atm m}^3 \text{kg}^{-1} \text{K}^{-1}$]
C_0	dimensionless constant in Fig. 6	r	radius [m]
C_i	constants with various units, sometimes temperature dependent ($i = 1-8$)	s	distance [m]
k	permeability [m^2]	T	temperature [K]
k'	apparent permeability [m^2]	V	fluid velocity [m s^{-1}]
L	length of test section [m]	Z	pressure parameter [atm kg m^{-3}].
M	molecular weight [kg mol^{-1}]	Greek symbols	
m	mass flow rate [kg s^{-1}]	λ	mean free path of gas molecule [m]
P	pressure [atm]	μ	dynamic viscosity [$\text{kg m}^{-1} \text{s}^{-1}$]
		ρ	density [kg m^{-3}].

pendent upon such properties as porosity, pore size distribution, and surface area, among others.

For higher velocities and greater mass flow rates, it is found that another term must be added to Darcy's equation to accurately represent theoretical and experimental data. Thus we obtain the Forchheimer equation

$$-\frac{dP}{ds} = \frac{\mu V}{k} + \rho BV^n \quad (2)$$

where n is a number close to 2 and ρ is the gas density. With this equation and the new material constant B it is possible to predict the flow of fluids through porous media over a wide range of flow conditions for both liquids and gases. The constant B , according to theory, should depend only on the porous medium and not on the fluid flowing through that medium [10].

The two right-hand terms in equation (2) have been designated the viscous term and inertia term, respectively. Theory suggests that the second term can be associated with the pressure loss due to repeated expansions, contractions, and direction changes experienced by the fluid due to its complex motion and the orientation of the pores and channels [10].

Thus equation (2) contains two constants which depend only on the porous medium regardless of the fluid involved. The accumulated data indicate that this equation correlates a wide range of data for a variety of porous media. However, it was observed [10] that the equation fails when applied to gas flow under certain conditions, e.g. larger values of k were obtained for gas flow than those obtained for liquid measurements and the k value varied for each gas. This difference was attributed to the 'slip' conditions present when gas flows through the small passages of low porosity media. Even at atmospheric pressure the slip phenomenon is observed for pore sizes small enough, i.e. of the order of the mean free path of the gas. The effect of slip in gas flow is to reduce the pressure drop below what might be expected, giving

k values higher than those for the no-slip condition. Slip is not observed for liquid flow, thus the lower values of k are obtained. Due to this slip phenomenon the actual permeability k should be replaced with an apparent permeability k' defined by

$$k' = k(1 + C_1\lambda) \quad (3)$$

where λ is the mean free path of the gas molecules and C_1 is a constant. From kinetic theory

$$\lambda = C_2 \frac{\mu}{P} \sqrt{\left(\frac{T}{M}\right)} \quad (4)$$

where T is the temperature, P the pressure and M the molecular weight of the gas. C_2 is a constant.

This result has been frequently tested over large pressure ranges, but always near room temperature. Using equation (4) for a specific gas at different pressures but constant temperature permits equation (3) to be written as

$$k' = k \left(1 + \frac{C_3}{P}\right). \quad (5)$$

This formulation has been used in a number of experimental studies with good results.

This investigation studied the influence of temperature upon the apparent permeability, at 1 atm using four gases. The results are correlated, using the gas properties shown in equation (4), by means of

$$k' = k \left(1 + C_4 \mu \sqrt{\left(\frac{T}{M}\right)}\right). \quad (6)$$

In addition, the temperature dependency of B , the material constant in the second term of equation (2) was determined.

Experimental work

Test sections consisted of porous aluminum oxide in the shape of hollow circular cylinders. The gases tested flowed from the hollow interior radially outward through the porous walls. The ends of the

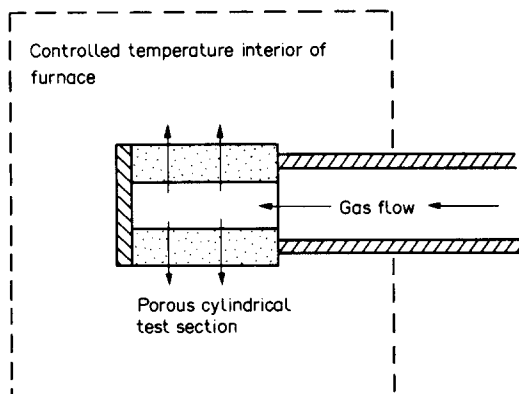


FIG. 1. Test section mounted in a controlled environment of a laboratory furnace. Gas enters the test section and flows radially outward through porous walls. The inlet tube and test section end plate are a non-porous ceramic.

cylinder were non-porous so there was no flow in the axial direction (Fig. 1), resulting in essentially one-dimensional flow with minimum edge effects. The test sections were mounted in the interior of a precision, high-temperature, laboratory furnace which provided a controlled temperature environment of ± 1 K over a large temperature range. To extend the temperature range below room temperature some data were taken with the test sections mounted in the interior of a freezer unit.

The physical properties of aluminum oxide are well suited for this type of experiment. The material can physically withstand the large temperature range used and will remain chemically neutral even at very high temperatures. Also, the thermal expansion is so low that there was only a very small expansion over the large temperature range tested.

Eight test sections were used with a porosity range of 38.1–49.8%. Lengths of the test sections ranged from 0.0234 to 0.1134 m. Outside diameters ranged from 0.0110 to 0.0161 m and inside diameters ranged from 0.0064 to 0.0123 m.

The temperature for each test section varied from 255 K to a peak temperature of up to 1520 K. The upper temperature for each test section was that associated with the section's mechanical failure; differences were noted in this temperature for the various test sections. The pressure was always very nearly 1 atm with a measured high of 1.12 atm inside the test section to a low of 0.95 atm on the outside.

The gases used were air, nitrogen, helium, and argon. Mass flow rates ranged up to 4.6×10^{-5} kg s $^{-1}$.

Flow equations

It was advantageous to replace the velocity in equation (2) by the mass flow, m . They are related by the simple relationship

$$m = \rho VA \quad (7)$$

where A is the area through which fluid flows at any radius r . For the cylindrical test section of length L

$$A = 2\pi rL. \quad (8)$$

Also

$$ds = dr \quad (9)$$

and

$$\rho = \frac{P}{RT}. \quad (10)$$

Substituting equations (7)–(10) in equation (2) and letting $n = 2$ gives

$$-\frac{dP}{dr} = \frac{\mu RTm}{kP2\pi rL} + \frac{BRTm^2}{P4\pi^2 r^2 L^2}. \quad (11)$$

Separating variables and integrating at constant temperature and mass flow rate yields a pressure parameter Z

$$Z = \frac{P_1^2 - P_2^2}{RT} = C_5 \frac{\mu}{k} m + C_6 Bm^2 \quad (12)$$

where

$$C_5 = \frac{1}{\pi L} \ln\left(\frac{r_2}{r_1}\right) \quad (13)$$

and

$$C_6 = \frac{1}{2\pi^2 L^2} \left(\frac{1}{r_1} - \frac{1}{r_2}\right) \quad (14)$$

are constants for a given test section, and r_1 and r_2 are the inner and outer radii, respectively. Equation (12) served as the working equation.

Experimental procedure

The apparent permeability and parameter B at various temperatures were determined by the following procedure. The temperature of the furnace controlling the test section environment was set at the desired level. The gas being tested was allowed to flow through the system to purge it of any remaining gases from earlier runs. The flow system consisted of a high precision coiled-capillary mass flow meter, followed by a filter for removing contaminants that could effect the flow characteristics of the porous material, a non-porous entrance tube of sufficient length within the furnace to assure the constant uniform gas temperature required for each measurement, and a precision manometer. When steady state was reached and the system fully purged, data were recorded. The mass flow rate of the gas was varied and the pressure drop through the porous test section was recorded. The temperature of the furnace was then changed, and when steady state was again achieved, a new series of mass flow rate–pressure drop data was taken.

With the temperature held constant the pressure parameter Z was plotted against the mass flow rate

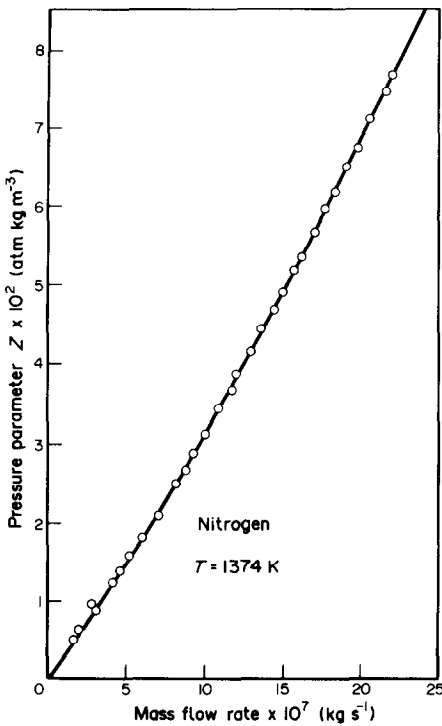


FIG. 2. Z vs mass flow rate for nitrogen at 1374 K. The apparent permeability k' of this test section-gas pair, at this temperature, is found from the slope at zero mass flow rate. Porosity, 45.7%.

m. The plot for nitrogen, Fig. 2 is illustrative. A least-square mathematical curve representing the results is of the form

$$Z = C_7 m + C_8 m^2. \quad (15)$$

The derivative of Z is

$$\frac{dZ}{dm} = C_7 + 2C_8 m \quad (16)$$

and the first term, through equation (12) is equal to

$$C_7 = C_5 \frac{\mu}{k}. \quad (17)$$

Thus knowledge of the slope of Z at zero mass flow rate (C_7), the geometrical properties of the test section (C_5), and the gas viscosity μ , yields a value for k' for each temperature. In addition, the regression fit of the curve provides the value of B at each temperature.

RESULTS

Results are shown in Figs. 2-6. Figure 2 is a typical curve obtained from plotting the data of one experimental run through one test section. A second-order curve fits the data with the two resulting terms providing information on the apparent permeability

k' and the material parameter B for this particular temperature.

Values of k' at various temperatures given in Fig. 3, show the dependence of the apparent permeability k' on temperature for each gas. For air, nitrogen, and argon the results are quite similar, while helium stands apart. Scatter in the data of air and nitrogen is about $\pm 3\%$, while the argon data is within 6%. Results for the other test sections are similar.

Expressing the apparent permeabilities in dimensionless form, by dividing by the value for the same gas at 300 K, gives the results shown in Fig. 4. Here the data scatter for air, nitrogen, and argon is about $\pm 5\%$ with the helium data within 11%.

The variation of the material constant B with temperature is shown in Fig. 5. The value of the second term of equation (2) is only 2-8% of the first term. Therefore, the scatter in the results for B is much greater, being of the order of $\pm 15\%$. The data appear consistent for the three gases: air, nitrogen, and argon, but depart from the other three in the case of helium. The behavior of B with temperature for other test sections resembles that shown in Fig. 5.

Because the relevant fluid properties are explicitly accounted for it is held that constant C_4 in equation (6) is a function of the solid material only and independent of the gas. If this is true, C_4 values obtained when using the four gases should fall on the same curve and vary only with temperature. Due to the low thermal expansion coefficient for the ceramic used ($8.12 \times 10^{-6} \text{ K}^{-1}$) the total volume change over the temperature range 255-1520 K was only 1.03%. Thus the actual permeability of the porous media would be very nearly constant and essentially independent of temperature. This agrees with the manufacturer's specifications [12] and with the limited data available in the literature [1, 2, 6]. Taking the permeability k as constant, the values of C_4 are plotted as a function of temperature in Fig. 6; C_4 is made dimensionless by dividing it by the value of C_0 for nitrogen at 300 K. The scatter in the data of C_0 for air, nitrogen, and argon is $\pm 5\%$ while the helium data varies by as much as 20%. Here C_0 is defined as

$$C_0 = (C_4)/(C_4 \text{ for N}_2 \text{ at 300 K}). \quad (18)$$

The results for the three gases, air, nitrogen, and argon, which have non-polar molecules of about the same size, show good agreement. Helium, with its much smaller molecules, shows variation in flow characteristics from these other three gases. However, Figs. 4 and 6 suggest that if a material can be calibrated at room temperature with nitrogen or the actual gas of interest, the results can be applied at higher temperatures with a fairly high degree of certainty. The same might or might not be expected of gases with larger polar molecules, i.e. H_2O , NH_3 , or larger. This would be a good area for additional future data.

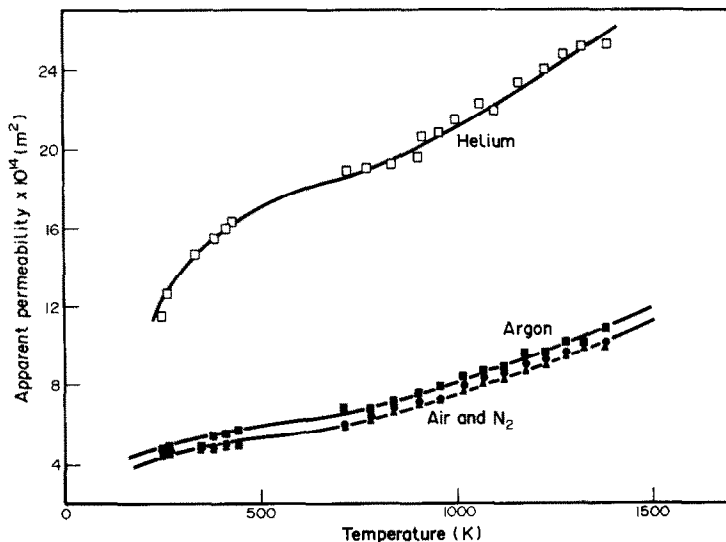


FIG. 3. Apparent permeability for one test section showing how helium data differs from the other gases. Porosity, 45.7%. Curves are typical for the sections tested.

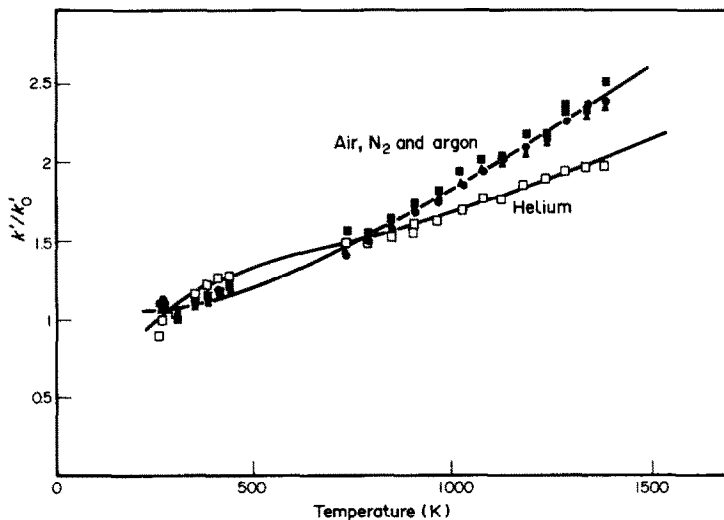


FIG. 4. Apparent permeability (dimensionless) k_0 at $T = 300$ K. Porosity, 45.7%.

CONCLUSIONS

The results of this work indicate that for gas flow through a porous aluminum oxide solid at 1 atm pressure, the major feature of the flow can be represented by equation (2) if the apparent permeability k' is used in place of k . The apparent permeability, k' , for an individual gas can be obtained for any temperature from Fig. 4 if it is known for that gas at 300 K. The apparent permeability for any gas can also be obtained from equation (6) and from Fig. 6 if the porous media can be calibrated with nitrogen at 300 K and 1 atm pressure.

For pressures other than 1 atm, equation (6) should be changed to

$$k' = k \left(1 + C_4 \frac{P_0}{P} \mu \sqrt{\left(\frac{T}{M} \right)} \right) \quad (19)$$

where P is the pressure in atmosphere and P_0 is a pressure of 1 atm.

REFERENCES

1. L. Grunberg and A. H. Nissan, The permeability of porous solids to gases and liquids, *J. Inst. Petrol.* **29**, 193-225 (1943).
2. J. C. Calhoun, Jr. and S. T. Yuster, A study of the flow of homogeneous fluids through ideal porous media, *A.P.I. Drill. Prod. Prac.* 335-355 (1946).

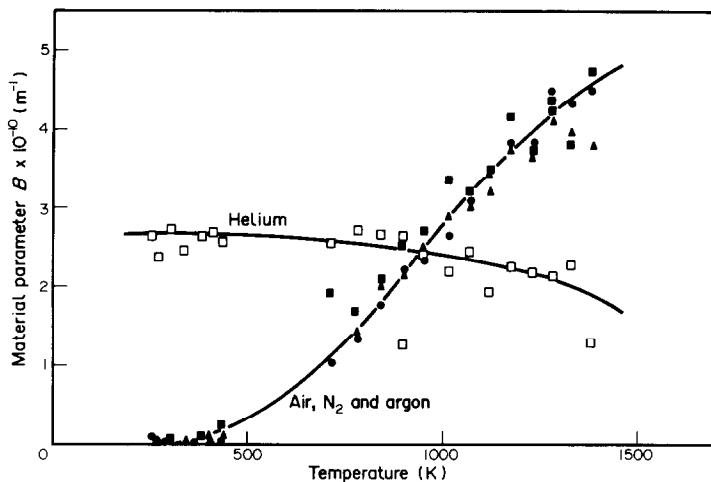


FIG. 5. Material constant B vs temperature. Porosity, 45.7%.

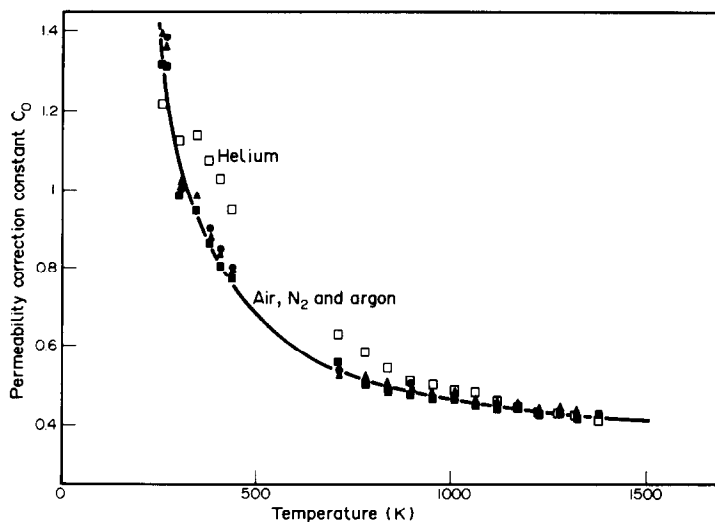


FIG. 6. Dimensionless permeability parameter C_0 from equation (18) vs temperature. Helium data varies slightly from the other gases. Porosity, 45.7%.

3. L. J. Klinkenberg, The permeability of porous media to liquids and gases, *A.P.I. Drill. Prod. Prac.* 200–213 (1941).
4. W. D. Rose, Permeability and gas-slippage phenomena, *A.P.I. Drill. Prod. Prac.* 209–219 (1948).
5. H. Krutter and R. J. Day, Modification of permeability measurements. *Oil Weekly* 104, 24–32 (1941).
6. M. B. Biles and J. A. Putnam, Use of consolidated porous medium for measurement of flow rate and viscosity of gases at elevated pressures and temperatures, *NACA Tech. Note* 2783 (1952).
7. P. C. Carman, Diffusion and flow of gases and vapours through micropores I. Slip flow and molecular streaming, *Proc. R. Soc. London A* 203, 55–74 (1950).
8. D. B. Greenberg and E. Weger, An investigation of the viscous and inertial coefficients for the flow of gases through porous sintered metals with high pressure gradients, *Chem. Engng Sci.* 12, 8–19 (1960).
9. T. W. Johnson and D. B. Taliaferro, Flow of air and natural gas through porous media, U.S. Dept. Interior Bureau of Mines Tech. Paper No. 592 (1938).
10. A. E. Scheidegger, Hydrodynamics in porous media. In *Handbuch der Physik*, VIII/2, pp. 625–662.
11. F. A. Schwertz, The structure of porous materials from gas penetration rates, *J. appl. Phys.* 20, 1070–1075 (1949).
12. Coors Porcelain Company, Bulletin No. 864.

EFFET DE LA TEMPERATURE SUR LA PERMEABILITE D'UN MATERIAU POREUX

Résumé—On étudie expérimentalement l'effet de la température sur l'écoulement de fluides compressibles à travers des matériaux poreux consolidés. L'étude couvre un domaine de température 255–1520 K à une pression de 1 atm. Le milieu poreux est une céramique d'alumine avec une porosité comprise entre 38,1 et 49,8%. Les gaz concernés sont l'air, l'azote, l'hélium et l'argon. En particulier est étudié, l'effet du terme correctif de "glissement" utilisé pour expliquer le changement de perméabilité dans les équations de l'écoulement. Ce terme dépend du libre parcours moyen du gaz et devrait augmenter avec la température. Aussi la perméabilité observée devrait être différente pour chaque gaz, à cause de la dépendance du libre parcours moyen, vis-à-vis du diamètre moléculaire, selon la théorie cinétique. Les deux hypothèses sont trouvées en harmonie avec les hypothèses microscopiques. Des graphes sont donnés montrant la relation entre la perméabilité et la température pour les quatre gaz. On montre aussi comment les paramètres du matériau poreux varient avec la température.

DER EINFLUSS DER TEMPERATUR AUF DIE PERMEABILITÄT EINES PORÖSEN MATERIALS

Zusammenfassung—Der Einfluß der Temperatur auf die Strömung eines kompressiblen Fluids durch verdichtete poröse Medien wurde im Bereich von 255 bis 1520 K bei einem Druck von 1 atm experimentell untersucht. Das poröse Medium war keramisches Aluminiumoxid mit einem Porositätsbereich von 38,1 bis 49,8%, die untersuchten Gase Luft, Stickstoff, Helium und Argon. Speziell wurde der Einfluß des "Schlupf"-Korrekturterms untersucht, der zur Erklärung der Änderung der Permeabilität in den porösen Strömungsgleichungen benutzt wird. Dieser Permeabilitäts-Korrekturterm hängt von der mittleren freien Weglänge des Gases ab, und man würde erwarten, daß er mit der Temperatur anwächst. Auch sollte die beobachtete Permeabilität infolge der Abhängigkeit der mittleren freien Weglänge vom Moleküldurchmesser gemäß der kinetischen Gastheorie für jedes Gas verschieden sein. Diese beiden Erwartungen wurden als vereinbar mit den mikroskopischen Annahmen befunden. Die Beziehung zwischen Permeabilität und Temperatur wird für die vier Gase in Diagrammform dargestellt. Das Verhalten von Helium weicht von dem der anderen drei Gase ab. Es wird ebenfalls dargestellt, wie sich die Parameter des porösen Materials mit der Temperatur ändern.

ВЛИЯНИЕ ТЕМПЕРАТУРЫ НА ПРОНИЦАЕМОСТЬ ПОРИСТОГО МАТЕРИАЛА

Аннотация—Экспериментально изучено влияние температуры на течение газов через отвердевшие пористые среды. Опыты проводились в диапазоне температур от 255 до 1520 К при давлении 1 атм. В качестве пористой среды использовался алюмосиликат с пористостью 38,1–49,8%. Исследования проводились на воздухе, азоте, гелии и аргоне. В частности, изучалась роль поправочного члена, учитывающего скольжение и используемого для объяснения изменения проницаемости в уравнениях, описывающих течение в пористом теле. Эта поправка к проницаемости зависит от среднего пути свободного пробега газа и предполагается, что она возрастает с увеличением температуры. Кроме того, проницаемость должна быть различной для разных газов из-за зависимости среднего пути свободного пробега молекул от их диаметра. Обе эти зависимости согласуются с положениями кинетической теории. Представлены графики, зависимости проницаемости от температуры для четырех газов. Поведение гелия отличается от поведения трех других газов. Показано также, как изменяются параметры пористого материала с температурой.